Drying shrinkage microcracking in cement-based materials

J. Bisschop
Geological Institute, ETH Zentrum, 8092 Zürich, Switzerland (jan.bisschop@erdw.ethz.ch)
Formerly at Microlab, Delft University of Technology

J.G.M. van Mier
Institute for Building Materials, ETH Hönggerberg, 8093 Zürich, Switzerland
Formerly at Microlab, Delft University of Technology

In this paper the nature of drying shrinkage microcracking in a variety of model cement-based materials, as well as in more practical types of concrete is described. The model mixtures were studied to elucidate the mechanisms of drying shrinkage microcracking and the factors that influence these mechanisms. This fundamental knowledge is important for the development of microstructural models that predict concrete behaviour. The degree and evolution of drying shrinkage microcracking in concrete have been determined with an eye on the durability of drying concrete. It has been determined however, that under the given experimental conditions, drying shrinkage microcracking remained superficial and did not occur in the bulk of the dried concrete.

Key words: Drying shrinkage, microcracking, concrete, microscopy, durability

1 Background of research

The doctoral work summarized in this paper was part of the interfaculty research program *'Micromechanics for macroscopic lifetime optimisation'* (DIOC-10) at Delft University of Technology. This program aims in developing a generic approach to describe and predict failure of a wide range of materials and constructions on basis of micromechanics. The failure process of many materials is related to structural imperfections of the material. Such defects can either be present in the materials in its "as-delivered state", or can form during service life of the material/construction. Micromechanics can play an important role in predicting those conditions that make defects grow from its initial state to the dimensions leading to failure of the materials and constructions.

In the present study it was tried to describe initial defects in concrete. Concrete is a heterogeneous material that may contain different types of initial defects. For example, air-bubbles, microcracks, and porous zones may all initiate stress concentrations upon loading, and may ultimately be the source of concrete failure. This study focused on the formation of initial defects (i.e., microcracks) in concrete caused by drying shrinkage. As drying shrinkage is a time-dependant deformation process, drying shrinkage microcracks are not only initial, they may also develop in course of time as drying progresses. The mechanisms, degree, and evolution of drying shrinkage microcracking in

concrete are hardly known. As stated in the state-of-the-art report [1] of the RILEM technical committee (TC-122-MLC) on microcracking and life-time performance of concrete "it would be highly desirable to carry out some systematic work on how a system of microcracks develops over time under particular environmental conditions". The research reported in this paper aimed at elucidating the nature of drying shrinkage microcracking in concrete. The degree and evolution of shrinkage microcracking in concrete should be known in order to say something about the durability of drying concrete, i.e., the long-term effect of shrinkage microcracking on mechanical and permeability behaviour. Moreover, fundamental knowledge about drying shrinkage microcracking in concrete is required for the development of microstructural concrete models. An example of such models is the combined mechanical lattice and lattice gas model developed by Jankovic et al. [2].

2 Introduction

Concrete, or more generally cement-based materials, are materials that consist of aggregates embedded in a matrix of hardened cement paste. Extraction of moisture from the cement paste pores by drying leads to shrinkage of the material. Drying shrinkage in hardened cement-based materials can easily lead to stresses and cracks, when the shrinkage is restrained. Concrete can be externally restrained by forces acting on the surface of a concrete element. This type of restraint is well known in civil engineering practice, since it can cause unwanted cracking in certain types of applications. This paper is not about (micro)cracking due to external restraints, but focuses on microcracking due to so-called internal restraints in the material itself. Internal restraining is an intrinsic property of shrinking concrete, and two types can be recognized: self-restraint and aggregate restraint. It should be mentioned that both types of internal restraints also occur when the concrete is externally restrained. In this research, however, we focused on microcracks due to internal restraint only, and therefore we studied microcracking in externally free shrinking specimen.

Self-restraint is the result of the shrinkage gradient caused by the development of a moisture gradient perpendicular to the drying surface. Microcracking due to self-restraint had been predicted to occur by e.g., Bazant and Raftshol [3] and Granger et al. [4] and it has been observed by Hwang and Young [5]. Self-restraint causes microcracks orientated mainly perpendicular to the drying surface and with a limited depth. The potential of aggregate restraint to be a crack-forming mechanism depends on factors like the magnitude of matrix shrinkage and the ratio in elastic modulus of the aggregates and the matrix. Goltermann [6] predicted microcracking by aggregate restraint and showed that it would lead to microcracks perpendicular to the grain boundaries. Bond cracks may possibly occur by aggregate restraint in certain configuration of aggregates. However, in the case of one aggregate particle embedded in a shrinking matrix radial compressive stresses occur around the particle that do not allow bond crack opening [6].

Observations of microcracking due to self-restraint and aggregate restraint have hardly been reported in literature. On the one hand, this possibly means that this type of microcracking is not common in concrete. On the other hand, it also might have to do with the difficulties that exist in detecting these types of microcracks in concrete. Direct visualization of microcracks in concrete (on

a cross-section) is not straightforward. Microcracks are easily introduced during the preparation (cutting and secondary drying) of the microscope sample, since concrete is rather brittle and very sensitive to changes in moisture content. In literature there have been discussions about whether microcracks seen in microscope samples of concrete are real, or "artifacts" introduced by sample preparation [7,8]. In this study the microcracks were impregnated with a fluorescent epoxy before cutting, therefore there was no risk of recording artificial cracks. This technique will be described in this paper. Next to microscopy, Nuclear Magnetic Resonance (NMR) and Acoustic Emission (AE) monitoring have been used to gain insight into the mechanisms of drying shrinkage microcracking. Concrete is a strongly heterogeneous composite material containing a range of types, shapes and sizes of aggregates. Also, drying shrinkage microcracking in concrete is caused by combined stresses of self-restraint and aggregate restraint. For these reasons it is difficult to study drying shrinkage microcracking in practical concrete. In order to study both mechanisms separately and to isolate the factors that determine the importance of both mechanisms, drying shrinkage microcracking was described in simple "model" cement-based materials. As will be explained in this paper it is possible to design mixtures in which microcracking due to aggregate restraint strongly dominates over microcracking due to self-restraint. Microcracking due to self-restraint only was studied in plain cement paste.

The present study focused on the effect of aggregates on drying shrinkage microcracking. It was hypothesized that the degree of drying shrinkage microcracking is mainly determined by the importance of aggregate restraint. This is because self-restraint causes microcracks with limited depth from the drying surface, whereas aggregate restraint can in principle cause microcracking in the bulk/core of concrete. Thus, the factors that determine the importance of aggregate restraint are probably also the factors that determine the degree of drying shrinkage microcracking in concrete. The main factors that were studied were: aggregate size, aggregate quantity, aggregate elasticity, aggregate angularity, bond strength, and aggregate grading. In practical concrete these factors are more or less fixed to fulfill all economical, mechanical, and durability requirements. Thus, the importance of aggregate restraint probably hardly varies between concretes. However, from a modeling point of view it is important to know how the above mentioned factors contribute to aggregate restraint. This paper will finish with a description of the degree and evolution of microcracking in more realistic concrete.

3 Materials and conditioning

3.1 Materials

In the studied model cement-based composites only factors concerning the aggregate content were varied, whereas the matrix composition was held constant. The matrix of the composites as well as the studied plain cement paste consisted of CEM I 52.5 R cement with a water-cement ratio of 0.45. The chemistry of the cement is given in [9]. The cement was sieved using a sieve with 0.3 mm holes to remove the larger agglomerates of cement grains. All specimens were made from the same cement batch. Using a w/c-ratio of 0.45, the viscosity of the cement paste was high enough not to cause segregation of the larger and heavier model aggregates used in this study. Still the paste was

"wet" enough to make composites with high aggregate contents sufficiently workable. Also, a w/c-ratio of 0.45 is high enough to avoid a significant influence of autogenous shrinkage. For example, in [10] it was shown that for cement paste with approximately the same cement composition and a w/c-ratio of 0.4 the autogenous shrinkage after 7 days is negligible.

In plain hardened cement paste no aggregate restraint occurs, and therefore this material was extensively used to study drying shrinkage microcracking by self-restraint only. In cement-based composites drying shrinkage microcracking is due to superimposed stresses caused by self-restraint and aggregate restraint. In a first series of experiments the effect of aggregate size on drying shrinkage microcracking was studied. In these experiments mono-sized and spherical glass spheres were used as model aggregates (see Section 6). It was found that in composites with mono-sized 6 mm aggregates, aggregate restraint caused much more microcracks than self-restraint. Therefore, this composite type was used to study the effect of variables concerning the aggregate content: aggregate elasticity, aggregate angularity, and bond strength. The effect of aggregate elasticity was studied in different composites containing mono-sized spheres of materials with varying elastic parameters (see Section 8). The effect of aggregate angularity and bond strength was studied in composites with mono-sized gravel grains or roughened glass spheres (see Section 9). Next to this rather fundamental study, drying shrinkage microcracking in a practical concrete is described. The sensitivity of drying shrinkage microcracking to the type of aggregate grading was tested by varying this factor (see Section 10). The composition of the various studied composites are given in the next sections. The quantity of aggregates in the composites is indicated with the aggregate volume percentage (V_a) and the quantity of matrix is given by the matrix volume percentage (V_m).

3.2 *Casting and curing*

After adding the water to the cement, the cement paste was stirred for 3 minutes in a Hobart mixer. Aggregates were mixed with the cement paste manually for 3 minutes. The mixtures were cast in prismatic moulds of 40x40x160 mm3. The filled moulds were vibrated for 10-40 seconds on a vibrating table depending on the workability of the mixture [9]. No significant differences in air-void contents were observed between mixtures vibrated for different durations [9]. Thereafter, the moulds were sealed with three layers of plastic foil sheets and stored for 24 hours at room temperature. Then, the specimens were weighed and placed in calciumhydroxide saturated tap water for 6 days at room temperature. The specimens were cured for 7 days (incl. first day sealed in mould) to develop a reasonable strength. For all mixtures, it was found that the water absorption (the weight of the water taken up by the specimen) during the 6 days wet-curing to be approximately 2.5% of the initial paste (matrix) weight content. The specimens were placed in water to avoid any shrinkage and cracking during hardening.

At an age of 7 days, the specimens were removed from the water and their weight was recorded after removing the water drops from the specimen surfaces with a dry cloth. Immediately after weighing all sides, except the top-surface of the specimens, were sealed with three layers of adhesive tape. The top-surface was the former (flat) bottom surface of the specimen in the mould. Only one side of the specimens was exposed to drying to create one-dimensional drying. After sealing,

the initial weight of specimens (including the tape) was recorded. Then, the specimens were placed in an environmental cabin to start the drying experiment. The environmental cabin (a Lab-line® Environ-Cab™) was ventilated with air with a temperature of 31.0°C ± 0.5°C and relative humidity of 31% ± 3%. These drying conditions were severe compared to "natural" drying, but were chosen because these conditions were expected to lead to more microcracking. It was thought that trends in cracking would be more clearly shown when there was more extensive cracking, which was beneficial for the objective of this study.

Drying shrinkage in cement-based materials is a slow, time-dependent deformation. As will be shown in this paper, drying shrinkage microcracking is in many cement-based materials also a time-dependent process. In order to compare drying shrinkage microcracking in different types of cement-based materials in non-equilibrium drying conditions, the degree of drying should preferably be the same. When this is the case it is easier to give mechanical explanations for the microcrack observations. In this study the matrix as well as the drying conditions were held constant and therefore the nature of *non-uniform* drying among composites did not vary significantly. This made it possible to define a so-called degree of drying concept [9]. The degree of drying is defined as the moisture loss expressed as a percentage of initial moisture content (excluding water absorption). Drying shrinkage microcracking was recorded at three degrees of drying: 10%, 20% and 30%, which corresponded roughly to 2 weeks, 2 months, and 5 month drying, respectively. The moisture loss (i.e., degree of drying) was monitored by frequent weight measurements. At the required specimen weight, the specimen was impregnated and the drying shrinkage microcrack-pattern was "frozen" into the material when the epoxy had hardened. The variation in drying behaviour among specimens was small and shown to be not the origin of the observed variation in microcracking. The drying curves of all composites can be found in [9].

4 Crack detection and quantification

4.1 Microcrack detection

In this study optical microscopy has been mainly used to detect microcracks in dried specimens. Specimen cross-sections had to be examined in order to measure the degree and depth of microcracking. This means that optical microscopy becomes "destructive" and this has two major disadvantages for the detection of drying shrinkage microcracks. Firstly, cutting of the (microcracked) material to produce the cross-section can easily introduce "artificial" microcracks [8]. Moreover, subsequent (secondary) drying of the cross-section surface (i.e., microscope sample surface) will unavoidably lead to the introduction of new microcracks [7,8]. Secondly, a specimen can only be used to determine the degree of cracking at one stage of drying. Therefore, the determination of the evolution of microcracking is cumbersome in comparison to a non-destructive technique, like for example the Acoustic Emission (AE) technique. With AE it is, however, much more difficult to study geometrical aspects of microcracking in detail. In this study, optical microscopy has been used to study long-term evolution of microcracking (i.e., 10%, 20%, and 30% degrees of drying). The initial short-term evolution of microcracking has been recorded with AE for two types of cement-based materials. Details on the AE monitoring conditions can be found in [11].

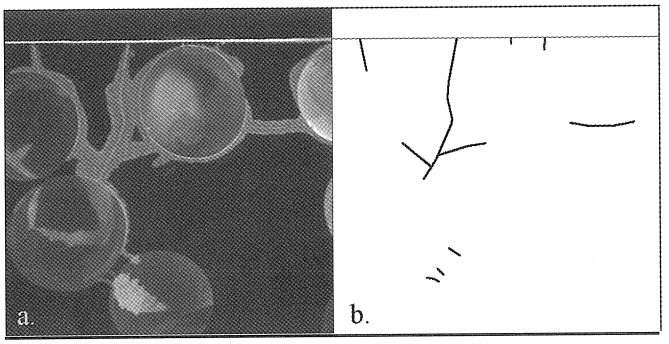

Figure 1: (a) Micrograph showing impregnated drying shrinkage microcracks (at degree of drying of 10%) at a cross-section of a composite with 4-mm glass spheres as aggregates. Micrograph taken in fluorescent light mode of optical microscope. (b) Manual traced cracks: no bond cracks were plotted. Image height is 11 mm.

To avoid recording artificial microcracks with optical microscopy, the crack-patterns were impregnated with a fluorescent epoxy before cutting the specimens. After hardening of the epoxy the crack-pattern was "frozen" into the material. A possible introduction of artificial microcracks during microscope sample preparation was not problematic because the cracks were not impregnated and thus were not recorded. The epoxy was sucked into the material under vacuum. By using this method only microcracks connected to the drying surface, either directly or indirectly by other microcracks, can be impregnated. It has been made likely that in the case of drying shrinkage microcracking, all impregnated cracks are in fact all microcracks present in the material [9]. Also, it has been shown that the effect of vacuum drying on the crack-pattern is probably negligible. A fluorescent dye was added to the epoxy to provide the microcracks and impregnated cement paste with a large contrast, especially in the UV-light mode of the optical microscope (see Fig. 1). After polishing the cross-sections, they were digitally recorded with a CCD camera on a Leica reflected light microscope at low magnification and in an UV-light mode.

4.2 *Microcrack quantification*

In spite of microcracks showing a good contrast to the surrounding material, it was in general not possible to identify cracks from the digital micrographs by means of digital image processing. Therefore, the microcracks were manually mapped on a printout (reference map) of the digital microscope recordings while sitting behind the microscope examining the specimens. The traced microcracks were redrawn on the computer screen with a mouse to obtain a digital crack map. No bond cracks were drawn in the crack-maps, because their presence is hard to judge for several reasons [9]. The manual crack-tracing leads to a simplified representation of the crack-pattern. Only large scale tortuosity as seen in Fig. 1 was traced. The small scale tortuosity, as shown for example in the inset of Fig. 2a, was ignored. For the purpose of this research this simplification sufficed. Of each specimen four cross-sections were made along the longitudinal axis of the specimen. Of each cross-section a crack-map of 40x40 mm was made from the center of the cross-section. In the crack-

maps in this paper, the crack-patterns on the four cross-sections are combined in a single figure to show trends in cracking more clearly.
The microcracks in digital crack-maps were automatically quantified using image analysis software. Crack-pattern parameters that were recorded were the cumulative length of cracks (TCL) in a crack-map and the maximum crack depth (MCD) of the crack-pattern. In the crack-maps presented in this paper trends in degree and depth of cracking are generally directly visible. Therefore quantitative data (i.e., TCL and MCD) are generally not given, but can be found in [9]. However, the overall orientation of microcracking will be given quantitatively. The orientation is shown in a simple crack-orientation diagram, the construction of such diagram is explained in [9,12]. The overall orientation of microcracking is thought to give a rough insight into the contributions of self-restraint and aggregate restraint in causing microcracking. In the case of cracking due to self-restraint only, cracks are orientated roughly perpendicularly to the drying surface. In that case the crack-orientation diagram will have a very elongated shape. In the case of cracking due to aggregate restraint only, it can be expected that the crack-orientation diagram has a round shape, as this type of cracking has a random orientation [6]. A composite with cracking due to superimposed self- and aggregate restraint will have a crack-orientation diagram with a shape in between of the two end-cases. The crack-orientation diagrams shown in this paper show the average value for the four sections. The total average crack length in specimens can be determined by adding the numbers in the four different directions.

It should be mentioned that the measured total crack length (TCL) on a cross-section is not a direct measure of the degree of microcracking in the specimen. Firstly, TCL does not include bond cracking. Secondly, the relationship between crack length and crack surface depends on the orientation of the crack surfaces, and these orientations may vary between specimens. More details on the crack detection, crack mapping, crack quantification methods, as well as the relation between crack length and crack surface can be found [9].

5 Drying shrinkage microcracking in plain cement paste

Drying shrinkage microcracking in plain hardened cement paste was studied to describe the self-restraint crack-forming mechanism. Under the given experimental conditions, drying shrinkage led to single or branched microcracks in plain hardened cement paste. Most microcracks had an orientation roughly perpendicular to the drying surface (Fig. 2a). The maximum observed crack depth was 12 mm. For branched microcracks also the upper portions of the microcracks were generally perpendicular to the drying surface, while the branches had a strong inclination to the drying surface (Fig. 2b). In cases where the branches were parallel to the drying surface, the crack depth was typically 3-5 mm. Quantitative data about the degree of microcracking in cement paste can be found in [9]. Drying shrinkage microcracks in plain cement paste are a result of self-restraint only. Self-restraint causes tensile stresses orientated parallel to the drying surface and as a result many microcracks make right angles with the drying surface. Crack branches inclined or parallel to the drying surface can be explained by the curl tendency of the non-uniform shrinking cement paste, which locally causes tensile stresses inclined to the drying surface.

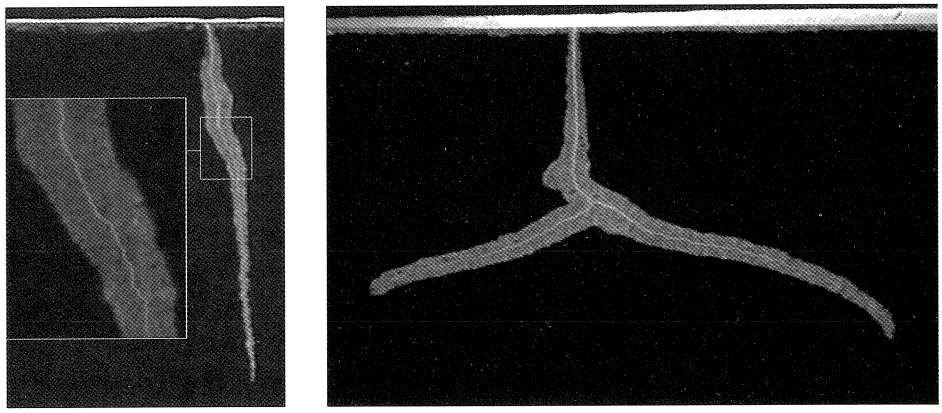

a. b.

Figure 2: Impregnated drying shrinkage microcracks on cross-sections of plain hardened cement paste at 10% drying. Micrographs taken in fluorescent light mode of optical microscope. (a) Microcrack perpendicular to the drying surface. Inset shows microscale tortuosity of the microcrack. Image height is 9.0 mm. (b) Branched microcrack. Image size 10.4 x 6.7 mm. Notice that the cement paste adjacent to the cracks is also impregnated.

Fig. 3 shows the evolution of drying shrinkage microcracking in plain cement paste in the first 13 days of drying (drying started after 7 days curing). It can be seen that most acoustic emissions occurred in the first hour of drying. Thereafter, only relatively few AE events were recorded, and the cumulative energy graph shows that the events after 1 hour drying were of small magnitude. These small events could possibly be related to small vibrations caused by moisture movement in the material [13]. No long-term evolution of microcracking was observed with optical microscopy

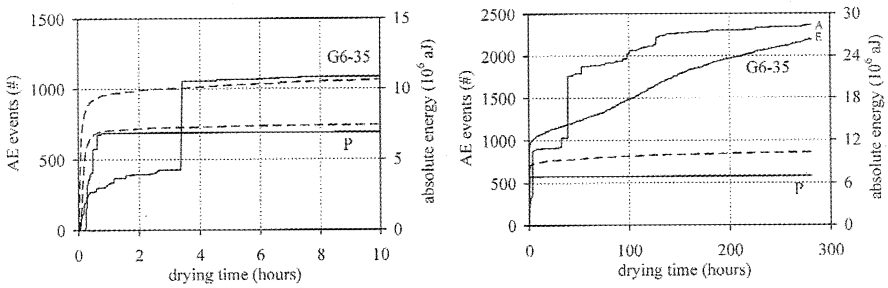

Figure 3: Evolution of Acoustic Emission in plain cement paste P and composite G6-35 (see Section 6) in first 10 hours (a) and first 280 hours drying (b). Dotted lines show cumulative number of AE events and solid lines show the cumulative energy associated with these events. In (b) the events curve is indicated with an E and the absolute energy curve with an A for composite G6-35. Info on the AE monitoring conditions can be found in [11].

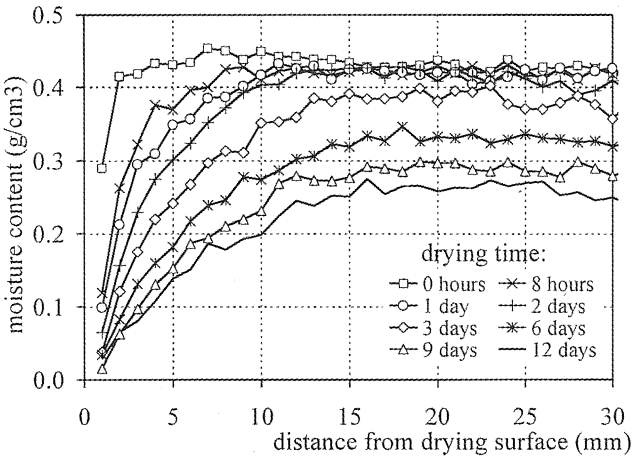

Figure 4. NMR moisture profiles showing the moisture distribution in plain cement paste.

as shown by the quantitative data obtained at 10%, 20% and 30% drying (after approx. 5 months drying) (see [9]). The early evolution of microcracking was explained by the development of the moisture gradient that was measured with Nuclear Magnetic Resonance (NMR) (see Fig. 4). Details about the NMR experiments can be found in [9]. It should be mentioned that the drying conditions in the NMR experiments were not the same as in the microcrack experiments. At the onset of drying the overall moisture gradient was probably largest (Fig. 4) and probably decreased already after 1 hour drying. As soon as the moisture gradient decreased cracking stops. Although it took about 2 days before the drying front reached the bottom of the specimen (Fig. 4), it was probably the decrease in the overall moisture gradient, instead of the depth of the moisture gradient that determined crack evolution in plain cement paste.

6 Effect of aggregate size on drying shrinkage microcracking

6.1 Studied composites

The effect of aggregate size on drying shrinkage microcracking was studied in simple cement-based composites with mono-sized glass spheres as aggregates. Glass spheres have been used as model aggregates, because they are spherical and have constant composition. They are commercially available in small size ranges. This allows the glass spheres to be used to study the effect of aggregate size on shrinkage microcracking. Also, they have approximately the same elastic properties as natural aggregates, like quartz gravel and sand, which make them a valid substitute for aggregates in real concrete. Five types of composites were prepared with five different sizes of glass spheres, relevant to aggregate sizes in practical concretes. In the composite name the capital refers to the aggregate type (G for glass in this case). The number in front of the dash indicates the diameter of the glass spheres in the composite. The exact average diameters of the glass spheres were: 0.54, 1.1, 2.3, 3.8, and 5.9 mm for the G.5, G1, G2, G4, and G6 glass spheres, respectively. The

quantity of aggregates in the composites is given by the aggregate volume percentage (V_a) and its value is shown by the number behind the dash in the composite name. The effect of aggregate size was studied in composites with a constant V_a of 35% and an accompanying matrix volume percentage (V_m) of 65%. This means that the number of aggregates in the composites decreased with increasing aggregate size. The glass spheres were perfectly smooth (see Fig. 9a) and the bond strength between the matrix and the spheres is considered to be very low. This was inferred from the fact that sectioned glass spheres easily felt out from the material after sawing the specimens.

6.2 Drying shrinkage microcracking

The effect of aggregate size on drying shrinkage microcracking is shown in Fig. 5. It can be seen that the total cumulative length and depth of microcracking increased with increasing aggregate size. In composites with 6 mm spheres (see Fig. 8) the degree of microcracking was unproportionally large in comparison to composites with smaller spheres. The overall orientation of microcracks was more random in composites with larger spheres. Self-restraint causes tensile stresses directed

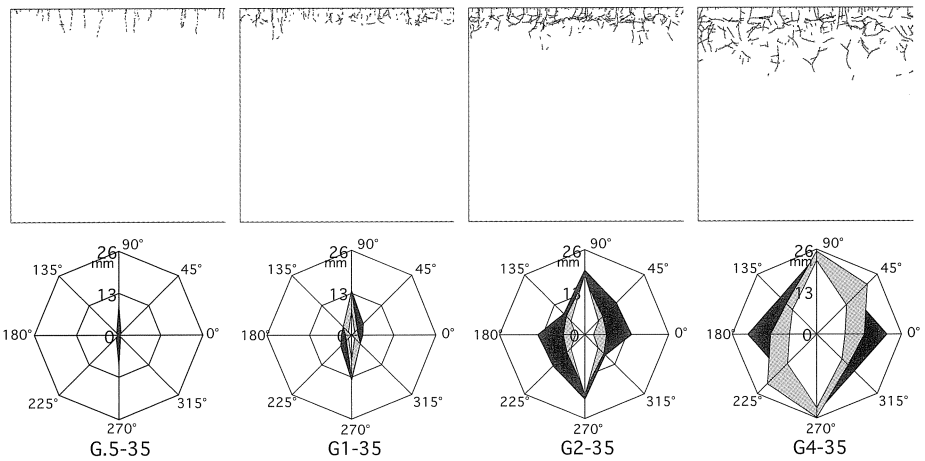

Figure 5: Effect of aggregate size on drying shrinkage microcracking in composites with glass spheres. Crack-maps (40x40 mm) showing cracking on 4 superimposed cross-sections (top-side was drying surface) at 30% drying and corresponding crack-orientation diagrams at 10% (white), 20% (light grey), and 30% (dark grey) drying.

parallel to the drying surface, whereas aggregate restraint causes tensile stresses with random orientation. Therefore, the increase of crack length and depth in combination with an increase in randomness of crack-orientation was a result of higher aggregate restraint in composites with larger aggregates. Microcracking not only became more randomly orientated with sphere size, it also became more random at 20% and 30% degree of drying, respectively, in composites G1-35 to G6-35. This makes it likely that long-term evolution of microcracking was a result of aggregate restraint. Composite G.5-35 showed microcracks with a strong preferred orientation similar to microcracking observed in plain cement paste, indicating that self-restraint was the main source of their forma-

tion. As a result no long-term evolution (similar as in cement paste) was found in composite G.5-35, because cracking due to self-restraint only occurred in the first hour of drying (see Fig. 3). Self-restraint also played a role in microcracking in the composites with larger spheres, because microcracking showed a preferred orientation in directions perpendicular to the drying surface, especially in the upper part of the specimens. But again it can be said that self-restraint was mainly active in an early period of drying (< 10% degree of drying), because microcracks formed after 10% dying had a rather random orientation. This was also shown by the evolution of acoustic emission in composite G6-35 (see Fig. 3). This composite showed a relatively strong AE activity (i.e., number of events) in the first hour of drying similar to the evolution in cement paste as a result of self-restraint. The AE activity in composite G6-35 after 1 hour drying is likely to be caused by microcracking by aggregate restraint only. Fig. 6 shows a micrograph of microcracking in composite G6-35.

6.3 Discussion

A larger crack length in combination with more randomly orientated cracking for composites with larger aggregates, indicates that the degree of microcracking due to aggregate restraint increased with aggregate size. Goltermann [6] predicted that in the case of perfect bond the total radial crack width (and length?) around a restraining aggregate particle will increase with aggregate diameter. However, in the case of smooth glass spheres the bond is probably low and Goltermann's model may not be directly applicable. With increasing particle size, the length of the circumference increases with the diameter of the aggregate particle. The larger the particle, the longer the "cement ribbon" encircling the particle. The total shrinkage deformation is equal to $2\pi r\epsilon_s$, and increases for larger particles. Assuming a deformation criterion for crack initiation and propagation [14], and identical specific shrinkage strains for the matrix around larger and smaller particles, the cement

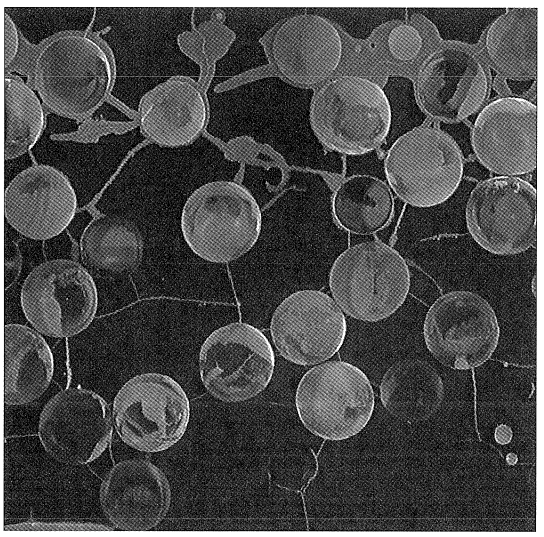

Figure 6: Micrograph of microcrack pattern in composite G6-35 at a degree of drying at 20% taken in fluorescent light mode of the optical microscope. Image size is 40 x 40 mm.

matrix will crack earlier (and more) when the particle size increases. Like in the case of perfect bonding the total radial crack width will be proportional to the aggregate size.

For smaller glass spheres higher shrinkage strains (i.e., longer drying times) are required before aggregate restraint cracking occurs, given a deformation limit for crack initiation. On basis of the observed moisture distributions (Fig. 4) it can be said that the rate of shrinkage decreased both in time and with depth into the specimen. The shrinkage strains that were reached at 20% drying in the lower half of composite G6-35 were large enough to cause aggregate restraint cracking at that location. For cracking to occur in the lower half of composites with smaller glass spheres higher shrinkage strains (i.e., higher degrees of drying) are required. The higher degree of drying required and the fact that the rate of shrinkage decreased in time, possibly led to increased importance of stress relaxation by creep of the matrix [15]. Stress relaxation will slow down crack formation. Thus, there might be an additional (indirect) effect of aggregate size on drying shrinkage microcracking.

7 Effect of aggregate quantity on drying shrinkage microcracking

7.1 Studied composites

The effect of aggregate quantity or aggregate volume percentage (V_a) on drying shrinkage microcracking was studied in composites with varying glass sphere sizes. It was found that the effect of V_a on the total length and depth of microcracking partly depended on sphere size. In this paper the effect of V_a in composites with 4 mm spheres will be shown as an example. The effect of V_a in composites with other spheres sizes is given in [9]. The effect of aggregate quantity was studied in composites with a V_a = 0% (i.e., plain cement paste), 10%, 21%, and 35%. In the composite name V_a is indicated by the number behind the dash, e.g., G4-35.

7.2 Drying shrinkage microcracking

The effect of aggregate quantity on drying shrinkage microcracking in the G4-composites is given in Fig. 7. In cement paste (P) microcracking is due to self-restraint only, and as a result cracks were orientated more or less perpendicular to the drying surface. The crack-orientation diagram shows a strong preferred orientation as a result. The presence of 4 mm glass spheres resulted in a higher degree of microcracking compared to cement paste, as a result of the additional stresses caused by aggregate restraint. The crack-orientation diagrams show that the randomness of crack orientations increased with aggregate quantity (at all stages of drying). Thus, the relative contribution of (tensile) stresses due to aggregate restraint (with respect to self-restraint stresses) increased with aggregate quantity. Also, the randomness of crack-orientation increased as a function of degree of drying, indicating that long-term evolution of microcracking was due to aggregate restraint.

The total cumulative length of the microcracking (the area of the crack-orientation diagram) increased with aggregate quantity up to a V_a = 21%. The degree of microcracking in G4-35 was, however, smaller than the one in G4-21. In composite G4-35, the higher degree of internal restraint provided by the higher number of aggregates was probably compensated by the lower quantity of

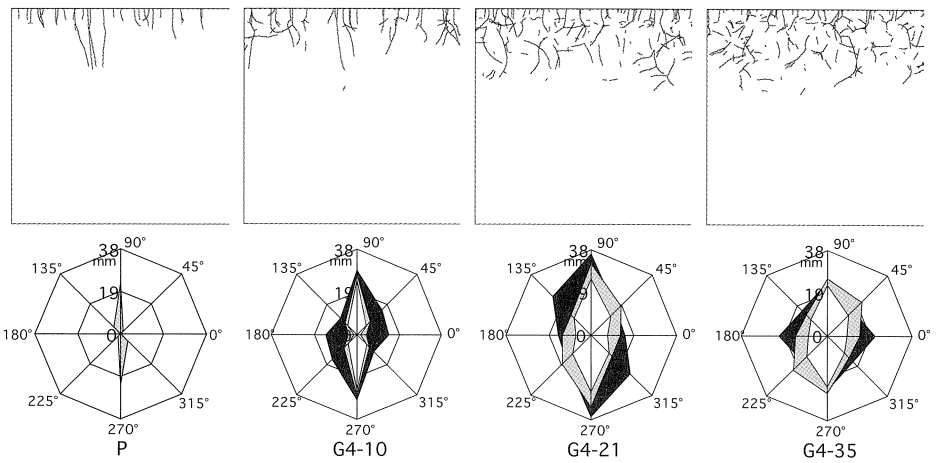

Figure 7: Effect of aggregate quantity on drying shrinkage microcracking in composites with 4 mm glass spheres and cement paste (P). Crack-maps (40x40 mm) showing cracking on 4 superimposed cross-sections at 20% drying (top-side was drying surface) and corresponding crack-orientation diagrams at 10% (white), 20% (light grey), and 30% (dark grey) drying.

shrinking paste (i.e., a lower degree of "driving force") or simply by the lower volume of matrix that can crack. The maximum depth of microcracking seemed not to be strongly affected by aggregate quantity in G4-composites.

8 Effect of aggregate elasticity on drying shrinkage microcracking

8.1 Studied composites

The elasticity of the aggregates and the matrix are expressed by the Bulk modulus of the aggregates (K_a) and the matrix (K_m), because aggregates embedded in a shrinking matrix can be considered to be more or less in a state of hydrostatic compression. The effect of Bulk modulus on drying shrinkage microcracking was studied in composites with aggregates having a lower K_a than the one for glass spheres (Polystyrene and Polypropylene spheres) and in composites with aggregates having a higher K_a than the one fore glass spheres (steel and ceramic spheres). As explained in Section 3.1 this was studied in composites with 6 mm aggregates, because in these composites the effect of aggregate restraint was most pronounced. No effect was found for aggregates with K_a larger than K_a of glass [9]. This can be explained from the fact that the K_a/K_m values are larger than 4 for these composites. Hobbs' rule predicts that the restraint provided by $K_a/K_m = 4$ is close to the restraint provided in the case of $K_a/K_m = \infty$ [16].

In this paper the effect of K_a smaller than K_a of glass will be described. The studied composites contained Polystyrene spheres (PS6-35), Polypropylene spheres (PP6-35), or glass spheres (G6-35). The elastic properties of the different aggregate types and the matrix are given in Table 1. The Young's

modulus of the glass spheres (E_a) was calculated on basis of the glass composition [9]. E_a of Polypropylene was taken from literature [17]. The Polystyrene spheres were foam plastic spheres of which the E_a and K_a are not known but are considered to be very low compared to Polypropylene, glass and the matrix. The modulus of elasticity of cement paste was measured on 40x40x160 mm3 specimens in compression at an age of 7 days. The Poisson's ratios of glass, Polypropylene, and cement paste were taken from literature [17,18]. The Bulk moduli were calculated from the elastic moduli and the Poisson's ratios.

Table 1: Properties of used spheres and cement paste.

material	sphere size (mm)	ρ (g/cm³)	E (GPa)	E_a/E_m	v	K (GPa)	K_a/K_m
Polystyrene	5.86 ± 0.23	0.023	?	<<0.1?	?	?	<<0.1?
Polypropylene	5.96 ± 0.01	0.86	2.0	0.1	0.41	3.5	0.3
glass	5.91 ± 0.15	2.48	77	4.7	0.23	47.5	4.4
cement paste	-	1.90	16.3	-	0.25	10.9	-

By choosing a more or less constant aggregate size and by keeping V_a constant at 35%, the behaviour of the composites could be compared directly to obtain the effect of aggregate elasticity. Both the glass spheres and Polypropylene spheres were spherical and had a smooth surface. The surface

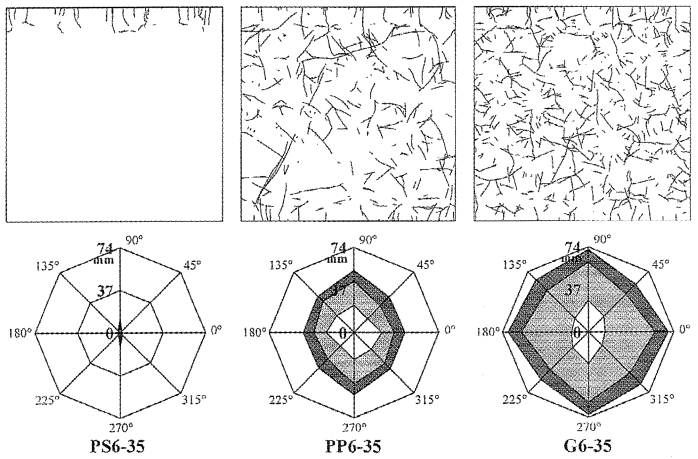

Figure 8: Effect of aggregate elasticity on drying shrinkage microcracking in composites with Polystyrene, Polypropylene, and glass 6 mm spheres. Crack-maps (40x40 mm) showing cracking on 4 superimposed cross-sections at 30% drying (top-side was drying surface) and corresponding crack-orientation diagrams at 10% (white), 20% (light grey), and 30% (dark grey) drying.

roughness of Polystyrene spheres is thought to be irrelevant, because these aggregates do not provide aggregate restraint.

8.2 *Drying shrinkage microcracking*

Fig. 8 shows the effect of aggregate elasticity on drying shrinkage microcracking. The Polystyrene particles did not provide significant aggregate restraint, because K_a/K_m was very small. Therefore all cracking in composite PS6-35 was due to self-restraint and as a result had a limited depth and did not show long-term evolution. Both, composites PP6-35 and G6-35 showed extensive microcracking due to aggregate restraint as shown by the degree, depth, orientation, and evolution of microcracking. The degree of microcracking in PP6-35 was significantly lower than the one of G6-35 at degrees of drying of 20% and 30%. Thus, for composites where $0.3 < K_a/K_m < 4.4$ the (limited) data indicate that the degree of drying shrinkage microcracking by aggregate restraint increases with increasing K_a.

9 Effect of aggregate angularity on drying shrinkage microcracking

9.1 *Studied composites*

Other factors that were thought to be important in drying shrinkage microcracking were the roundness/angularity of aggregates and the bond strength between aggregates and matrix. It was expected that these factors are especially important when microcracking is caused by aggregate restraint. A higher bond strength compared to the one of smooth spheres and an angularity as seen in natural non-spherical aggregates must in some way affect the development of drying shrinkage microcracking caused by aggregate restraint, as these factors hinder shrinkage of the matrix around aggregates. In this study a distinction is made between fine angularity and coarse angularity of aggregates. Fine angularity is the surface roughness of grains. Aggregates with a rough surface were expected to have a better bonding with the matrix than smooth aggregates. Fine angularity probably increases the physical bond strength between aggregate and matrix, because of an increased contact surface area in comparison to spherical, smooth aggregates. It is not expected that surface roughness will lead to increased chemical bonding. With coarse angularity the irregular shape of natural aggregates is meant, which in the present study was river (quartz) gravel and sand.

The effect of aggregate angularity was studied in composites with 6 mm aggregates, because it was thought that due to the important role of aggregate restraint, the effect would be most pronounced in this type of composite. To study the effect of aggregate surface roughness only, a composite with sandblasted (6 mm) glass spheres (in that case letter *r* is added in the composite name) was compared with a composite with smooth (6 mm) glass spheres. The difference in surface roughness is shown in Fig. 9. The effect of coarse angularity was studied by comparing a composite with natural aggregates to a composite with the same content of round spheres. The natural aggregates were made comparable to 6 mm glass spheres by keeping the (average) individual volume of the aggregate particles the same. It should be mentioned that there was some variation in surface roughness of the natural aggregates (see Fig. 9). Therefore, the effect of coarse angularity probably also includ-

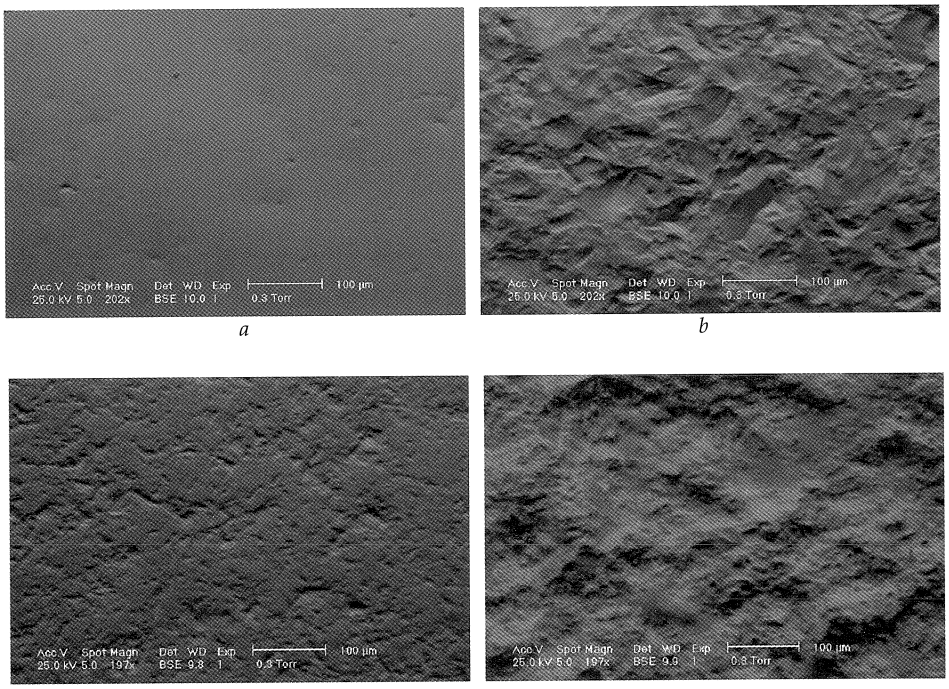

Figure 9: Surface morphology of a glass sphere (a); a sand-blasted glass sphere (b); natural aggregate with a rather smooth surface (c); natural aggregate with a rough surface (d). SEM-BSE images by A-B diode switching.

ed some effect of fine angularity. The modulus of elasticity of the sand grains was not measured, but can be expected to be not very different from the glass spheres, in view of the composition and the density of the mainly quartzitic sand grains. Also the values given in literature for river gravel and sand of 60 to 75 GPa [19] is close to the value calculated for glass (see Table 1).

9.2 *Drying shrinkage microcracking*

Fig. 10 shows the effect of aggregate angularity on drying shrinkage microcracking in composites with mono-sized 6 mm aggregates. Both, coarse and fine angularity led to a reduction in the degree and depth of microcracking, especially at 20% and 30% drying. In composite N6-35 the degree and depth of microcracking was slightly smaller than in composite G6r-35, probably because the natural aggregates showed both, coarse and fine angularity. The contribution of both factors in the reduction of degree and depth of microcracking could, however, not be determined. After a degree of drying of 20% no significant evolution in degree and depth of microcracking occurred any more in composites G6r-35 and N6-35, while cracking did not reach the bottom of the specimens. The reason for this has probably to do with the better bonding of aggregates and matrix, which caused stresses to be more evenly distributed in the matrix around the aggregates. Thus, the built-up of

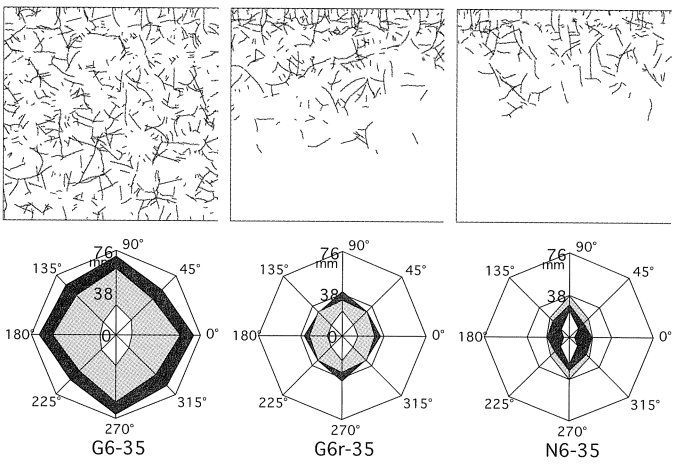

Figure 10: Effect of aggregate angularity on drying shrinkage microcracking in composites with smooth and sandblasted 6 mm glass spheres, and natural 6 mm aggregates. Crack-maps (40x40 mm) showing cracking on 4 superimposed cross-sections at 30% drying (top-side was drying surface) and corresponding crack-orientation diagrams at 10% (white), 20% (light grey), and 30% (dark grey) drying.

stress-concentrations was slower, and as a result stress-relaxation by creep of the matrix might have become more important and have reduced crack-evolution. Also, the degree of microcracking in composites G6r-35 and N6-35 may also have been less than in G6-35 due to a more difficult fracture propagation.

10 Effect of aggregate grading on drying shrinkage microcracking

10.1 Studied composites

To get insight into the degree and evolution of drying shrinkage microcracking in a rather practical concrete, a composite with Fuller graded natural aggregates and an aggregate volume percentage (V_a) of 59% was prepared. A V_a of 59% was found to be the highest content of graded aggregates for which still reasonable workability of the mixture was achieved for the given matrix properties (without using plasticizers). Also, the effect of grading type on drying shrinkage microcracking was studied. Apart from the composite with Fuller graded natural aggregates, two composites were prepared with two types of gap gradings. In Table 2 the grading compositions of the aggregates in the three composites are given. It should be mentioned that the maximum aggregate size of 6 mm is still rather small compared to practical concretes, but was chosen to keep the ratio between specimen size and aggregate size (i.e., 40/6) reasonable. The gradings are based on aggregates with a rather limited size ranges, instead of being based on the conventional sand size ranges used in concrete technology. The reason for this is that the composites with graded natural aggregates were

Table 2: Grading compositions.

aggregate size (mm)	Nfg-59 (wt-%)	Ngg1-59 (wt-%)	Ngg2-59 (wt-%)
0.5	18.3	38.5	38.1
1	17.6	-	-
2	17.5	-	30.7
3-4	26.3	-	-
6	20.3	61.5	31.2

made comparable to a series of composites with graded glass spheres with narrow size ranges (see Section 6). The results of the graded glass spheres composites are not reported in this paper but can be found in [9]. In [9] also a detailed description is given of how the narrow sand size ranges were obtained by sieving the conventional size ranges. Also, it is explained how subsequently the given Fuller and gap gradations in Table 2 were calculated. In the composite's names fg stands for Fuller graded and gg stands for gap graded.

10.2 Drying shrinkage microcracking

In Fig. 11 the effect of grading type on drying shrinkage microcracking in composites with natural aggregates is given. In the three studied composite types the degree and depth of microcracking were rather low compared to other composite types. The main reason for this behaviour is probably the lower matrix volume percentage V_m and the presence of more and graded restraining aggregates. Both factors reduced the shrinkage of matrix (with smaller graded aggregates) around the larger (6 mm) aggregates, and reduced shrinkage stresses. For all grading types, a large proportion of microcracking at a degree of drying of 10% was a result of self-restraint, because the crack-orientation diagrams shows a strong preferred orientation of cracking in directions perpendicular to the drying surface. After 10% drying, microcracking was likely to be a result of aggregate restraint, because this microcracking had a rather random orientation (see Fig. 11). The effect of grading type on degree and depth of microcracking is not clear and finding mechanical explanations for the observations is thought to be difficult on basis of the presented optical data only. Modeling might be adopted here.

10.3 Evolution of microcracking in concrete

Composite Nfg-59 is a realistic concrete with the exception of the maximum aggregate size and the rather stepped Fuller grading. Still, the evolution of drying shrinkage microcracking in composite Nfg-59 is thought to say something about the durability of drying concrete. It will determine the extent to which concrete disintegrates by drying in the course of time, and becomes more sensitive to the effects of mechanical loading or ingress of fluids and gasses. As shown in Fig. 11 there is a significant evolution in the degree of cracking in composite Nfg-59, as mentioned before probably as a result of aggregate restraint. The depth of cracking, which is also relevant for the durability of

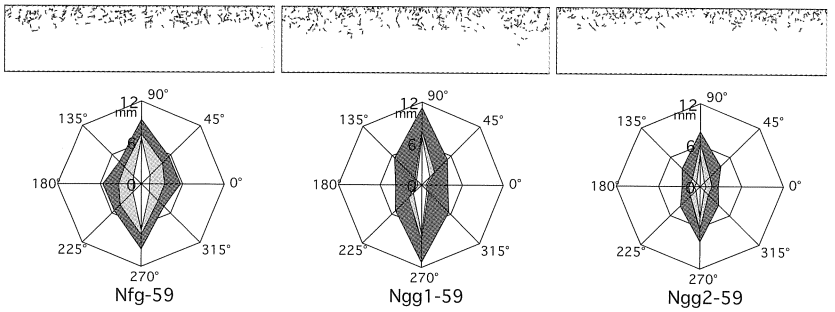

Figure 11: Effect of aggregate grading on drying shrinkage microcracking in composites with Fuller graded and gap graded natural aggregates (see Table 2). Crack-maps (10x40 mm) showing cracking on 4 superimposed cross-sections at 30% drying (top-side was drying surface) and corresponding crack-orientation diagrams at 10% (white), 20% (light grey), and 30% (dark grey) drying

concrete, did however not increase significantly. The question is what will happen after elongated drying time? This question will largely be answered by looking to the evolution of cracking in composite Gfg-59 which showed similar microcrack behaviour as Nfg-59 [9]. In this type of composite drying shrinkage microcracking was studied at drying degrees of 4%, 10%, 20%, 30%, and at the ultimate degree of drying (see Fig. 12). The ultimate degree of drying was obtained by drying a specimen at 105°C in a furnace until all evaporable water was removed [9]. This took about 7 days. In this way not only the ultimate degree of drying was reached, also a very high drying rate was achieved. Although these extreme drying conditions will never occur under practical circumstances, the cracking at the ultimate degree of drying is thought to be the absolute upper bound for crack-evolution. Note that at the ultimate degree of drying would be about 70% according the definition given in Section 3.2.

The evolution of microcracking in composite Gfg-59 is given in Fig. 12. It can be seen that TCL increased to about 50 mm at the ultimate degree of drying, and MCD reached about 6 mm. As mentioned in Section 10.2, it is the much lower V_m and the presence of a higher number of (graded) restraining aggregates that caused a much lower degree of cracking compared to for example composites G6-35, G6r-35 and N6-35. The crack-orientation diagram in Fig. 12 shows that cracking after 10% drying is likely to be caused by aggregate restraint, as cracks formed after 10% drying have a rather random orientation, especially after 30% drying. It might therefore be surprising why there is hardly any evolution of MCD in the graded composite and that no microcracking occurred in the bulk of the composites at the ultimate degree of drying. Again, this behaviour can probably be explained by stress-relaxation caused by creep of the matrix. The shrinkage rate will decrease in depth and time, and therefore creep becomes more and more important in the course of drying and will slow down crack formation. It is questionable, however, that this factor also played a role going from 30% to the ultimate degree of drying, because the drying duration of 7 days is probably too short for a significant creep effect.

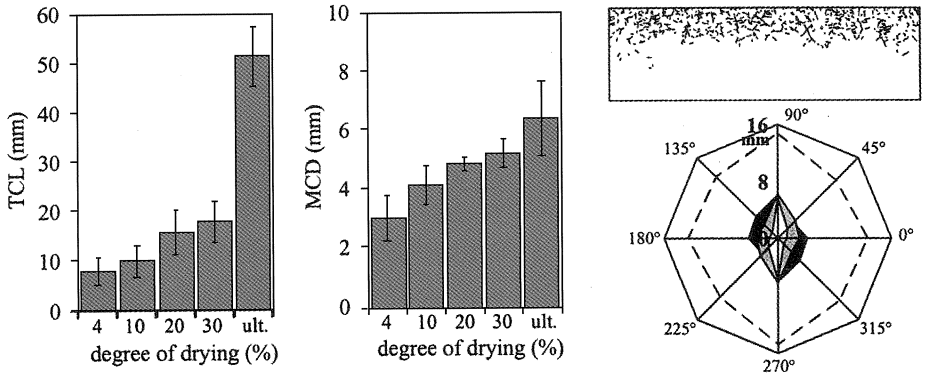

Figure 12: Crack evolution in concrete Gfg-59. (a) TCL and MCD as function of degree of drying. Standard deviation is given for the four cross-sections in one specimen. (b) Crack-map (40x12 mm) at the ultimate (ult.) degree of drying (4 combined sections) and crack-orientation diagram at 10% (white), 20% (light grey), and 30% (dark grey), and ultimate (dotted outline) degree of drying.

11 Conclusions

In this paper a phenomenological and quantitative description is given of drying shrinkage microcracking in cement-based materials due to internal restraints. Apart from a fundamental study on simple model mixtures to understand the mechanisms of this type of microcracking, the evolution of microcracking in more realistic concrete has been determined. The main conclusions that were drawn from this study are:

- At 31°C and 31% RH self-restraint in plain cement paste led to single microcracks orientated perpendicular to the drying surface and branched microcracks with an orientation roughly parallel to the drying surface. Microcracks caused by self-restraint appeared within the first hour of drying; no long-term evolution was observed in the studied specimens. This early evolution of microcracking was probably directly related to development of the moisture gradient, which was "steepest" in the first hours of drying.
- In composites containing round or angular aggregates up to a diameter of 6 mm, drying shrinkage microcracking was due to superimposed stresses caused by self-restraint and aggregate restraint. Like in cement paste, self-restraint in composites was active in the formation of microcracks in the initial stage of drying. The degree of drying shrinkage microcracking increased with aggregate size. The effect of aggregate quantity on drying shrinkage microcracking depended on aggregate size. The long-term evolution of microcracking observed in composites was likely to be caused by aggregate restraint.
- Lower Bulk modulus of aggregates in the range $0.3 < K_a/K_m < 4.4$, larger bond strength or more angular aggregates significantly reduced drying shrinkage microcracking in composites with 6 mm aggregates.

- In the studied concretes, drying shrinkage microcracking due to internal restraints remained superficial (crack depth < 8 mm) even in the ultimate state of drying and under extreme drying conditions. The effect of aggregate grading type on drying shrinkage microcracking seemed to be small. Further research is needed to find the degree of microcracking in concrete with a more practical specimen size and maximum aggregate size. Also, further research is needed to find the effect of the (superficial) microcracking on properties like strength and permeability. Such research will elucidate the effect of drying shrinkage microcracking on the durability of drying concrete.

12 Acknowledgements

The doctoral research summarized in this paper was part of the interfaculty research program *'Micromechanics for macroscopic lifetime optimisation'* (DIOC-10) financed by Delft University of Technology and was carried out in the Microlab at the Faculty of Civil Engineering and Geosciences. Dr. L. Pel and Dr. T. Shiotani are gratefully acknowledged for their help with the NMR and the AE experiments, respectively. The technical support of Mr. A.S. Elgersma throughout the project is strongly appreciated.

References

[1] Jensen, A.D. and Chatterji, S., State of the art report (RILEM TC-MLC-122) on microcracking and lifetime of concrete – part 1. Material and Structures 29 (1996) 3-8.

[2] Jankovic, D., Küntz, M., and Van Mier, J.G.M. Numerical analysis of moisture flow and concrete cracking by means of Lattice type models. In proc. of FraMCoS - 4, (R. de Borst, J. Mazars, G.Pijaudier and J.G.M. van Mier, eds.), Balkema, Rotterdam, (2001) 231-238.

[3] Bazant, Z.P. and Raftshol, W.J., Effect of cracking in drying and shrinkage specimens. Cement and Concrete Research 12 (1982) 209-226.

[4] Granger, L., Torrenti, J.M., and Acker, P., Thoughts about drying shrinkage: Experimental results and quantification of structural drying creep. Materials and Structures 30 (1997) 588-598.

[5] Hwang, C.L. and Young, J.F. Drying shrinkage of Portland cement pastes. I. Microcracking during drying. Cement and Concrete Research 14 (1984) 585-594.

[6] Goltermann, P., Mechanical predictions of concrete deterioration - Part 2: classification of crack patterns, ACI Materials Journal 92 (1) (1995) 58-63.

[7] Gran, H.C., Fluorescent liquid replacement technique. A means of crack detection and water:binder ratio determination in high strength concretes. Cement and Concrete Research 25 (2) (1995) 1063-1074.

[8] Bisschop, J and Van Mier, J.G.M., How to study drying shrinkage microcracking in cement-based materials using optical and scanning electron microscopy? Cement and Concrete Research 32 (2) (2002) 279-287.

[9] Bisschop, J. Drying shrinkage microcracking in cement-based materials. Ph.D thesis Delft University of Technology, the Netherlands, Delft University Press (2002). 208p.

[10] Tazawa, E., and Miyazawa, S., Influence of constituents and composition on autogenous shrinkage of cementitious materials. Magazine of Concrete Research 49 (178) (1997) 15-22.

[11] Shiotani, T., Bisschop, J., and Van Mier, J.G.M., Temporal and spatial development of drying shrinkage cracking in cement-based materials. Accepted for publication in Engineering Fracture Mechanics 70 (12) (2003) 1509-1525.

[12] Bisschop, J. and Van Mier, J.G.M., Effect of aggregates on drying shrinkage microcracking in cement-based materials. Materials and Structures 35, September-October (2002) 453-461.

[13] Shiotani, T, Bisschop, J., Van Mier, J.G.M., AE activity during drying processes in cement-based materials. Proc. 16th Int. Acoustic Emission Symposium (ed. T. Kishi et al.), Japan (2002) 290-297.

[14] Van Mier, J.G.M. and Nooru-Mohamed, M.B., Geometrical and Structural Aspects of Concrete Fracture. Engineering Fracture Mechanics 35 (4/5) (1990) 617-628.

[15] Mindess, S. and Young, J.F., Concrete. Prentice-Hall, Inc. Englewood Cliffs, N.J. (1981).

[16] Hobbs, D.W., The dependence of the bulk modulus, Young's modulus, creep, shrinkage and thermal expansion of concrete upon aggregate volume concentration. Materials and Structures 4 (20) (1971) 107-114.

[17] Van Krevelen, D.W., Properties of polymers. Third edition (Elsevier Science, b.v., 1997) 367-380.

[18] Simeonov, P. and Ahmad, S., Effect of transition zone on the elastic behaviour of cement-based composites. Cement and Concrete Research 25 (1) (1995) 165-176.

[19] Nilsen, A.U. and Monteiro, P.J.M., Concrete: a three phase material. Cement and Concrete Research 23 (1993) 147-151.